by Levy Ferreira Costa, Giovanni De Carne, Giampaolo Buticchi, and Marco Liserre

The Smart Transformer

A solid-state transformer tailored to provide ancillary services to the distribution grid

The solid-state transformer (SST) was conceived as a replacement for the conventional power transformer, with both lower volume and weight. The smart transformer (ST) is an SST that provides ancillary services to the distribution and transmission grids to optimize their performance. Hence, the focus shifts from hardware advantages to functionalities. One of the most desired functionalities is the dc connectivity to enable a hybrid distribution system. For this reason, the ST architecture shall be composed of at least two power stages. The standard design procedure for this kind of system is to design each power stage for the maximum load. However, this design approach might limit additional services, like the reactive power compensation on the medium voltage (MV) side, and it does not consider the load regulation capability of the ST on the low voltage (LV) side. If the SST is tailored to the services that it shall provide, different stages will have different designs, so that the ST is no longer a mere application of the SST but an entirely new subject.

Renewable Energy and the Power Distribution Grid

The integration of renewable energy systems and new loads, like electric vehicles (EVs), has changed the distribution grid. The grid, once passive and static with a limited number of distributed generators, is now active and dynamic. The LV grid hosts, together with residential and commercial loads, small generators in the range of hundreds of watts to a few hundred kilowatts. This generation capability consists of diesel generators, gas microturbines, photovoltaics, and micro wind turbines. Among these resources, there are the controllable ones (diesel and gas generators) and the ones called *renewables* that provide energy when available from natural sources (e.g., wind, sun irradiation, and tides). This last category has two main features: high power-injection variability and distributed presence in the distribution grid. These generation units vary their power-output with short-term forecast possibilities and at different times due to the different geographical distribution. The major challenges for the grid are the voltage control, frequency stability, reverse power flow, and protection systems coordination [1], [3].

The ST, an SST with control and communication functionalities, can represent a solution for many of the mentioned problems. The ST features cover a wide range of services, like the reactive power support in MV grids, dc connectivity at both the MV and LV levels, and load control in the LV side. The ST is designed following a three-stage solution, with the isolation stage in the dc/dc converter. This solution enables the galvanic isolation between the two grids, guaranteeing the appliances' safety during abnormal conditions (e.g., faults or lightning strikes). The ST basic design does not differ substantially from the SST concept. However, unlike the SST, which is designed mainly for traction applications or as a mere one-to-one replacement of conventional transformers, the ST shall be tailored to provide those previously mentioned services.

This article presents the grid-tailored design approach (GTDA) for STs, taking in account the load requirements (e.g., unbalanced conditions) and the services that can be provided to the grid (e.g., reactive power support). The

Digital Object Identifier 10.1109/MPEL.2017.2692381
Date of publication: 23 June 2017

2329-9207/17©2017IEEE

proposed design approach shows how the ST can be made smaller, thanks to the higher control capability on the LV side, and how the saving obtained due to such control actions on the LV side can be used to provide more services on the MV side.

The ST Concept

Several ST architectures have been proposed and classified in the literature. An overview of the possible architectures, presenting several configurations, has been previously published [4]–[7]. Among the possible configurations, the three-stage one (comprising an MV stage, a dc/dc stage, and an LV stage) enables dc-link connectivity and also guarantees input/output decoupling of voltages and currents, providing the system control more degrees of freedom and making it the preferred candidate for an ST. To handle the MV level involved on the power conversion, modular architectures bring several advantages, such as low dv/dt (low electromagnetic interference emission), the potential to use standard LV-rating devices, and modularity, which allows for the implementation of redundant strategies to increase fault tolerance and availability. For these reasons, modular architectures are preferable for ST applications. Figure 1 shows the grid scenario in which the ST should operate, i.e., MV to LV connection, with the availability of the dc links preferably in both sides.

LV Side

In the LV grid, the ST controls the voltage waveform. Independently from the load current request, the ST provides a sinusoidal voltage waveform with nominal amplitude and frequency. However, the ST can provide ancillary services modifying the voltage amplitude and frequency. It is well known that the load power consumption depends on the voltage magnitude and that the grid-connected generators have frequency/power droop controllers to sustain the grid frequency during perturbations. The ST exploits these characteristics for modifying load consumption and generator production in the LV grid. The possible ancillary services provided by these features are load identification and control [8], soft load reduction [9], reverse power flow limitation [10], [11], and ST overload control [12]. In the first service, the sensitivities of active and reactive power to voltage and frequency variations are identified. These sensitivities are employed to increase the control accuracy: when the ST receives a power reduction request, the voltage controller reduces the voltage amplitude by the amount needed to achieve the desired power reduction. This service, called *soft load reduction*, allows participation in the transmission grid control, offering a power absorption control range of ±10%. This is shown in Figure 2, where the LV-side control modifies the voltage to reduce the consumption on the LV side. An additional 10% of control capability is given by the possibility to modify the frequency, interacting with the renewables.

Considering theses services, the most suitable topologies to implement the ST from the power electronics viewpoint are voltage source inverter (VSI) four wires, based on the full-bridge (FB), T-type, or neutral-point clamped (NPC) topologies [4]. Due to the requirement of the neutral conductor, the middle-point dc link is available, leading to an additional voltage balancing circuit. The two-level FB topology represents the simplest approach and a consolidated solution. On the other hand, the three-level topologies have been accepted as feasible solutions by industry; for this reason, the NPC or T-type topologies would allow the use of 600-V devices, improving the output waveform and system efficiency at the same time.

dc/dc Conversion

The availability of two dc stages allows for the creation of local or regional dc grids. The MV dc link works as a connection point between STs and can host new loads, like fast-charging electric vehicle stations and distributed resources, large photovoltaic and wind power plants, and battery energy storage systems. The LV dc link offers instead the possibility to connect the dc loads directly to a LV dc grid, avoiding an intermediate conversion stage at the user's site. The dc links allow for the ac power flow separation between the MV and LV grids. This feature enables controlling the two grids independently, with only the constraint of the active power link. This power stage has strict requirements, such as high-rated power and high current capability on the LV side and high-voltage (HV) capability, high frequency isolation, and high efficiency on the MV side. The basic configuration implies series-connected modules in the MV side and parallel-connected ones in the LV side.

The basic module of the dc/dc stage is based on an isolated dc/dc converter, implemented normally using the dual-active-bridge (DAB) converter [13] or the series-resonant converter [14]. An additional approach is the use of multiwinding-based topologies, such as the quadruple-active bridge (QAB) [15] as a basic cell. This converter presents the same advantages as the DAB converter but with a lower number of high/medium frequency transformers. Following the configuration in [15], the converter has a lower number of auxiliary components (e.g., drivers, auxiliary power supply) in the LV side. Regardless of the basic power module, the LV dc link and/or the MV dc link are available for microgrid connections.

MV Side

At the MV level, the ST controls the active current to keep the MV dc link voltage constant at the nominal value. The reactive power is controlled separately from the active power and represents a degree of freedom for the system control. The ST can inject reactive power for voltage support purposes both in steady state, controlling the voltage profile in the grid, and during transients, offering services like LV ride-through. With the help of communication, the ST can perform power factor correction at the HV/MV substation, reducing the reactive power request to the

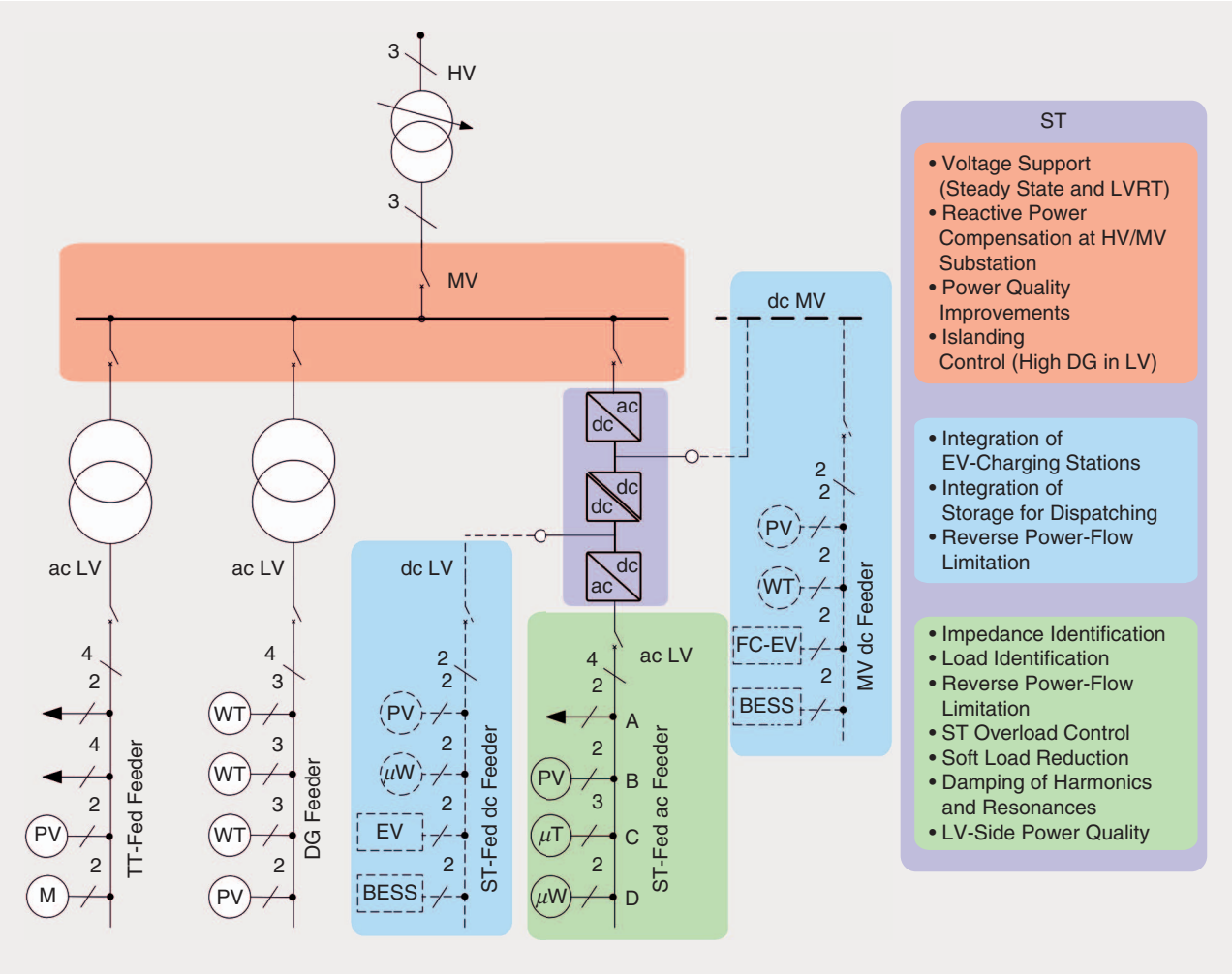

FIG 1 The ST and its role in the electric grid. TT: traditional transformer; PV: photovoltaic; M: machine; DG: distributed generation; BESS: battery energy storage system.

transmission grid. The active power is the only link between the ac MV and LV ST stages. Oscillating power components can be controlled separately from the active power. Thus, harmonic voltage and current compensation is possible.

The most promising topologies to implement the MV stage of the ST are the cascaded H-bridge (CHB) converter and modular multilevel converter (MMC). Both converters share the same features: modularity, possibility of fault-tolerance implementation, multilevel operation, reduced dv/dt, and filter size. On one hand, the MMC presents the additional advantage of providing the dc link for the connection of MVdc loads/sources. On the other hand, this topology requires a very complex control system, a bulky filter on the dc side (when compared to the CHB topology), and high cost. For these reasons, it has not been adopted for MV applications yet, but only in HV applications. The CHB represents the most promising topology solution, thanks to its advantages associated with a simple modulation and control system. Its main disadvantage, however, is the lack of an MVdc link for MVdc grid connectivity.

The NPC converter may provide a possible topology to implement the MV stage, and it represents a standard solution for MV applications. However, due to the voltage level of the MVdc link (normally more than 15 kV), series connection of an insulated-gate bipolar transistor (IGBT) is required. Furthermore, the NPC is not a modular solution, and a bigger ac filter (compared to the previous converters) must be installed.

SST Topology Selected for the ST

To select the proper architecture of the modular three-stage ST, not only must the power converter be chosen, but the number of modules also plays an important role. In this section, these points are discussed, and the ST architecture is selected, considering the grid specification provided in Table 1. Regarding the MV-side converter, the CHB topology is selected due to its simpler operation and control. On the LV side, a standard VSI is employed. The DAB and the QAB converters are considered for the dc/dc stage because they offer power flow control. The ST architectures employing DAB and QAB as a building block of the dc/dc solution are shown in Figure 3(a) and (b). The unit shown in this figure is a replaceable part of the ST, and it is composed of the dc/dc

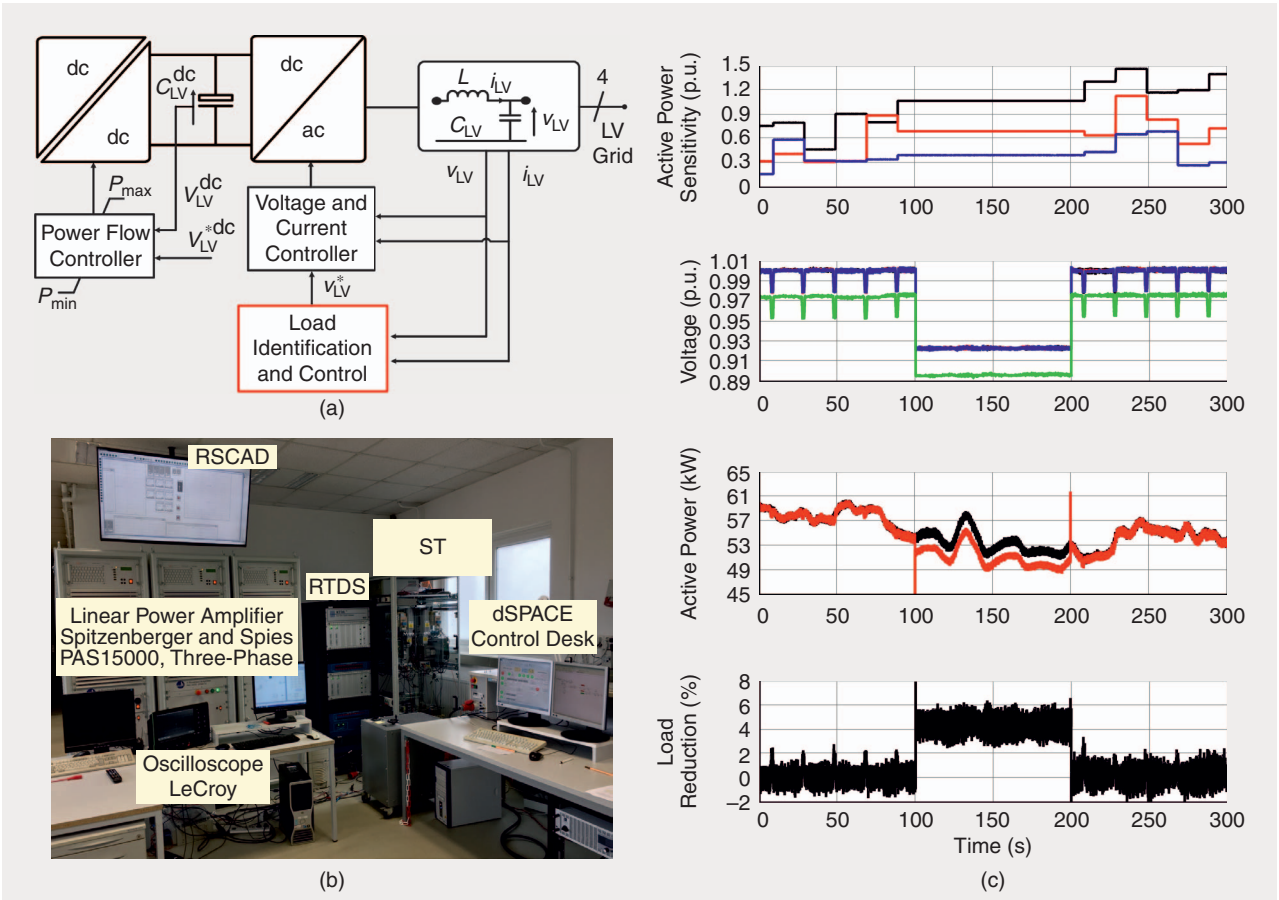

FIG 2 The services to the LV grid: (a) the block scheme of the LV-side control, (b) an experimental setup based on a real-time digital simulator (RTSD), and (c) the results of a soft load reduction experiment [8] showing, from top to bottom, sensitivity coefficients, voltage profiles, power profiles, and the percentage of shed load.

converter associated with the respective MV cell of the CHB connected to it.

Selecting the Number of Units

The constraints to selecting the number of modules are the fault tolerance capability, the IGBT blocking voltage, the system complexity, the number of components, and the rated power of the modules. All of these parameters influence the cost, reliability, efficiency, and system complexity. The number of units is selected from the MV-side viewpoint, using cost as the main parameter.

If a large number of modules is selected, the semiconductor-blocking voltage of the MV side is reduced, but the total number of parts (including the auxiliary power supply, drivers, and communication) and system complexity increase considerably. Table 2 shows the main parameters of the ST MV side for different numbers of units, considering both DAB and QAB solutions. In this analysis, the IGBT power module available on the market from the main semiconductors is summarized in Table 3. Notice that only dual configuration is assumed in this table. Table 4 presents the considered IGBT power module for cost analysis carried out in this article. These power modules are from Powerex, also with dual configuration. The cost was obtained directly with the manufacturer on 20 February 2017. For the cost analysis, IGBT modules from Powerex/Mitsubishi are assumed, as shown in Table 4. As detailed in Table 2, the MV-side current is independent from the number of units because the modules share the voltage and power among them in the MV side. Thus, the use of HV-blocking IGBTs implies an underutilization of the devices because they are normally available only for high current. Furthermore, the device cost is very high, leading to the most expensive solution, as shown in Table 2. From the cost analysis, the most advantageous solution is employing 27 or 36 CHB cells (with a difference of only US$720 between them). Considering also the implementation complexity and the number of components, 27 CHB cells represent the most suitable solution; this design is thus presented in this article.

Table 1. The grid specifications.

Rated power	MVac	LVac	Grid Frequency	Total MVdc Link	LVdc Link
1 MVA	10 kV	400 V	50 Hz	700 V	700 V

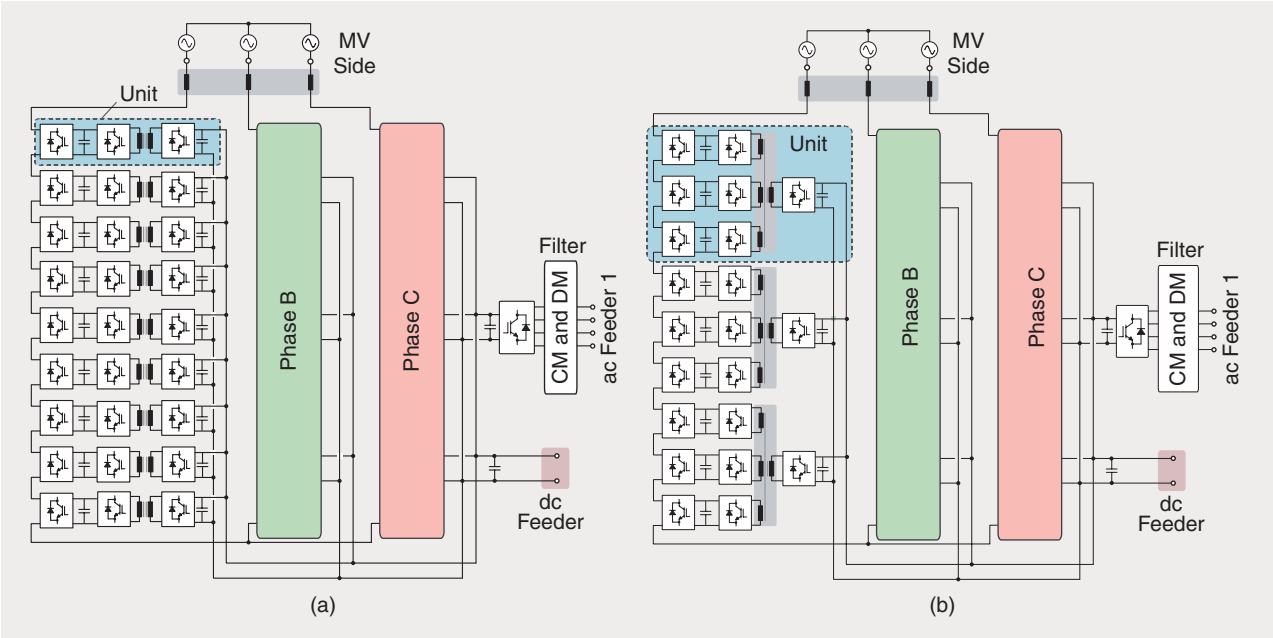

FIG 3 An ST architecture considering two dc/dc solutions: (a) DAB and (b) QAB. CM: common mode; DM: differential mode.

QAB and DAB Converter Comparison

Since the DAB and QAB converters are the most promising topologies, they are compared in this article in terms of cost, efficiency, complexity, and reliability. Both converters are designed assuming the specifications and parameters shown in Tables 1 and 2. A phase shift modulation is considered [15], with a nominal phase angle of 35° and switching frequency of $f_s = 20$ kHz. The detailed values obtained from the QAB design and DAB design, used in the comparative analysis of these converters, are presented in Table 5. A comparative analysis of both converters appears in Table 6, where the main parameters of the design are summarized, and the components quantity and cost are presented.

The QAB converter has fewer LV cells, as well as fewer transformers. Consequently, the employed semiconductors and auxiliary components, such as gate-driver units, auxiliary power supplies, and control and communication systems are also reduced compared to the DAB solution. Although higher current rating devices are required to implement the LV cell of the QAB (Table 6), the individual device cost does not differ much from the cost of the devices required by the DAB solution, as can be seen in Table 3. Consequently, the QAB converter presents the most effective solution both economically and practically, since it uses fewer components. By using QAB instead DAB, a cost saving of US$2,350.08 (only in semiconductors) is achieved; this value can be higher if the auxiliary components are considered. Figure 4 shows a qualitative comparison between the QAB and DAB converters. In a balanced condition, both converters present the same performance from the efficiency viewpoint [15]. On the other hand, the control of the QAB presents a higher complexity than the DAB one. Despite this fact, the QAB solution presents several advantages over the DAB solution; thus, we chose to implement the dc/dc stage of the ST.

Proposed Grid-Tailored Approach

ST design is a complex matter: the peak load consumption is difficult to evaluate, and it is limited in time to a few hours per year. The actual procedure for sizing of the conventional transformer is quite conservative and is based on the peak load. As highlighted in [16], this results in a transformer oversizing in most cases (63% in the study mentioned). Only a few transformers have been adequately sized or undersized.

Table 2. The main parameters of the MV side of the ST for different numbers of power units.

Number of Units		Unit Power Level (kW)		Number of CHB Cells	MV dc Link (kV)	IGBT Voltage Rating (kV)	Mean Current (A)	IGBT Current Rating (A)	Cost (US$)
QAB	DAB	QAB	DAB						
3	9	333.33	111.11	9	3.4	6.5	17.6	150	12,402
6	18	166.67	55.56	18	1.7	3.3		75	19,404
9	**27**	**111.11**	**37.04**	**27**	**1.13**	**1.7**		**50**	**6,480**
12	36	83.33	27.78	36	0.85	1.2		50	5,760
15	45	66.67	22.22	45	0.68	1.2		50	7,200

Table 3. The available IGBTs on the market, considering the main manufacturers.

Voltage Rating (V)	Manufacturer	Current (A)	Configuration	Part Number
6,500	Powerex	85	Dual	QIC6508001
	Mitsubishi	750	Single	CM750HG-130R
	Infineon	250	Single	FZ250R65KE3
3,300	Powerex	100	Dual	QID3310006
	Mitsubishi	1,000	Single	CM1000HC-66R
	Infineon	200	Dual	FF200R33KF2C
	Fuji	800	Single	1MBI800UG-330
1,700	Powerex	75	Dual	CM75DY-34A
	Mitsubishi	75	Dual	CM75DY-34A
	Infineon	150	Dual	FF150R17KE4
	Fuji	75	Dual	2MBI75VA-170-50
1,200	Powerex	50	Dual	CM50DU-24F
	Powerex	75	Dual	CM75DU-24F
	Mitsubishi	100	Dual	CM100DY-24NF
	Infineon	50	Dual	FF50R12RT4
	Infineon	75	Dual	FF75R12RT4
	Fuji	75	Dual	2MBI75VA-120-50

Table 4. The considered IGBT power module for cost analysis from Powerex and dual configuration.

MV Side				LV Side			
Voltage Rating (V)	Current Rating (A)	Reference	Cost (US$)	Voltage Rating (V)	Current Rating (A)	Reference	Cost (US$)
1,200	300	CM300DX-24S1	137.39	6,500	150	QIC6508001	689
	200	CM200DX-24S	145.01	3,300	100	QID3310006	539
	150	CM150DX-24S	110.37	1,700	75	CM75DY-34A	120
	100	CM100DY-24A	99.65	1,200	50	CM50DU-24F	80.31
	75	CM75DU-24F	98.55				
	50	CM50DU-24F	80.31				

The classic SST design is based on equally sized converters, and it stems from the sizing of conventional transformers. As a base case, the SST has been sized for 1-MVA power. The ST enables an improved load control, mainly on the LV side. Modifying the voltage amplitude and frequency, the ST can interact with the LV generators and loads to modify power consumption [9]. The possibility to reduce the active power consumption acting on the voltage is well known in North America, where the conservation voltage reduction (CVR) is widely applied [17], [18]. The CVR exploits the transformer online tap changers to decrease the voltage in the downstream grid. Upon reducing the voltage, the grid power consumption also decreases. In [15], the energy saved throughout the year is estimated to be 4%, and the load peak reduction is estimated to be up to 4%. However, the CVR cannot evaluate the power reduction online. The

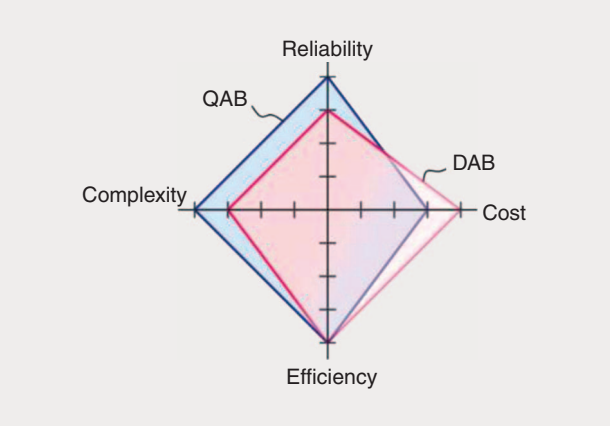

FIG 4 A qualitative comparison of QAB and DAB performance characteristics.

Table 5. The detailed values obtained from the QAB and DAB converter designs.

Parameters	QAB		DAB	
Number of Units	Nine (Three per Phase)		27 (Nine per Phase)	
Unit Power Level	111.11 kW		37.04 kW	
	LV Side	MV Side	LV Side	MV Side
dc-link voltage	700 V	1.13 kV	700 V	1.13 kV
Semiconductor voltage rating	1.2 kV	1.7 kV	1.2 kV	1.7 kV
Semiconductor mean current	84 A	17.6 A	28 A	17.6 A
Current rating	150 A	75 A	50 A	75 A
Selected semiconductor	CM150DX-24S	CM75DY-34A	CM50DU-24F	CM75DY-34A
Device cost	US$110.37	US$120	US$80.31	US$120
Basic cell cost	US$1,986.66	US$6,480	US$4,336.74	US$6,480
MFT root-mean-square (RMS) current	184 A	38 A	61 A	38 A
Required inductance (LV side)	17.3 uH		51.8 uH	

Table 6. A comparative analysis of the DAB and QAB converters.

	DAB	QAB	
Parameter	LV Side	MV Side	LV Side
Number of cells	27	27	9
IGBT current rating	50 A	50 A	150 A
IGBT voltage rating	1.2 kV	1.7 kV	1.2 kV
Number of semiconductors	108	108	36
Total semiconductor cost	US$4,336.74	US$6,480	US$1,986.66
Auxiliary power supply	27	27	9
Gate driver unit	54	54	18
Control and communications system	27	27	9
Number of MFTs	27	9	
Isolation requirement	10 kV (prim-sec)	10 kV (prim-sec) 1.2 kV (sec-sec)	
TOTAL COST	US$10,816.74	US$8,466.66	

prim: primary; sec: secondary.

ST, implementing the online load identification [8], can identify the load sensitivity to voltage and frequency variation and thus apply a more accurate control action, as shown in [9]. From the survey's result in [19], the distribution system operators identify the load response to voltage variations as a constant current load for the active power and as a constant impedance load for the reactive power. Considering the ST capability to reduce the voltage up to 10%, the amount of power reduced for a residential grid can be estimated to be 10% of active power and up to 20% of reactive power. Considering a power factor of 0.9 p.u., the total apparent power that can be controlled is 20%.

Power generation in the LV grid is independent from the voltage amplitude. The voltage control performed by the ST cannot modify the generators' power injection, as it is not sensitive to voltage variations. However, by controlling the frequency, the ST can interact with the droop controller of the distributed generators in the LV grid and modify their power injection [10], [12]. While a power reduction is technically feasible [10], increasing the power of the generators depends on the availability of controlled resources in the LV grid. The renewables do not usually have reserve energy to be employed in this case; thus, appliances like microturbines, diesel generators, or storage systems are needed for providing upwards regulation capability to the ST. The current LV grid takes the direction of implementing more controllable generation and load in the smart grid vision [20]. Although in few years the grid will be fully controllable, it can be assumed that the controllable generation installed in the LV grid can cover up to 10% of the load consumption.

Considering the ST features, a total apparent power controllability of 20% is estimated. Thus, the ST size can be decreased by 20% with respect to the conventional transformer design. In this context, an innovative ST design approach, the GTDA, is proposed. Applying the GTDA, the power converters of the ST are used in a more efficient way, resulting in cost and footprint reduction. On one hand, if more grid services are desired, a power converter stage may present higher cost, depending on the service. On the other hand, the savings in one or more stages can be used to compensate for the extra cost of the other stage (due to the additional service), keeping the total cost comparable to the one from the conventional design. The GTDA has the advantage of providing more services at the same cost of the SST or conventional transformer design.

As an example, the MV converter can be sized following two strategies: the minimum cost or the inclusion of more grid ancillary services. The minimum cost strategy designs the MV side depending on the dc/dc converter size, minimizing the hardware expenses. The second strategy is based on sizing the MV converter to provide services to the MV grid, such as reactive power support. In this case, the cost savings from the LV side and dc/dc stages can be invested on the MV-side stage, leading to a constant cost with the additional service of reactive power support. Table 7 shows the power level required for each ST stage, considering the different design approach. In this table, case A is the standard design approach, where each stage is designed for the same power, defined by the load. In case B, the load reduction service is applied in the LV, leading to a power reduction and consequently to cost minimization. In that case, all stages are designed for the same power level. In case C, the GTDA is considered, and the cost saved in the LV and dc/dc stages is invested in the MV side, to provide more reactive power to support the MV grid. These values are obtained based on the detailed design of the converters, including the calculation of the cost, as discussed in the next section.

GTDA Design Procedure

To design an ST using the GTDA, the topology shown in Figure 3(a), as well as the specifications depicted in Table 1, is used. The ST is designed considering the three cases shown in Table 7. For each converter, sizing is based on the semiconductor selection, cooling system, and capacitor bank (Table 8). These components are designed following (1)–(4).

Design Considerations

Semiconductor Design

The semiconductors are selected considering the maximum blocking voltage and the average current flowing through them. For each case shown in Table 7, the power processed by the converter is affected, but the voltage levels are constant. The selection is made based on the average current and the power dissipated in each device (1). For the power semiconductors selection, the available IGBT power modules from Infineon Technology (with dual configuration) are considered in the dc/dc and LV stages. For the MV stage, IGBT power modules from Infineon Technology and Fuji Electric are assumed. For price comparison purposes, the quotation is obtained from the same distributor (Mouser Electronics) and for the same number of pieces (40 pieces).

Cooling System Design

To design the cooling system of the power converter, the conventional approach based on the semiconductors' power dissipation (P), ambient temperature (T_{amb}), junction temperature (T_J), and thermal resistance in the power path between the junction and the ambient (R_{th}) is considered [21]. To evaluate the influence of the services on the cooling system, the cooling system performance index (CSPI) approach [21] is used. Using this approach, a constant cooling profile is selected, leading to a constant CSPI, as defined in (3). The volume of the heatsink is proportional to the power dissipation, as described in (4). To compute the cost of the cooling system, it is assumed that the price of the heatsink is proportional to the volume. A constant CSPI is considered to keep the junction temperature at 100 °C for the device with lower losses; i.e., a lower cooling system requirement. For the devices that dissipate more power, parallel heatsink blocks are considered.

Capacitor Bank Design

The required capacitance is calculated according to the power processed by the converter [22], using (2) in Table 8. The required capacitance is directly related to the apparent power processed for a given voltage ripple (ΔV_{MVdc}), and therefore it is directly influenced by additional grid services. For cost comparison, a basic capacitor block of 100 μF/500 V is assumed, to be assembled in series/parallel according to the converter requirements.

The design solution for the LV-side capacitor is based on setting the maximum voltage oscillation (i.e., 5%), employing (5). The capacitance is calculated taking in account the dc-link nominal voltage and the possible current imbalance that can happen in the grid. This value can be obtained from historical data of the LV grid and knowing in advance the presence of fixed three-phase loads (balanced by nature). If the peak-to-peak power oscillation is

Table 7. Case studies definition.

Design Cases		LV ac/dc (MVA)	dc/dc (MW)	MV (MVA)	Cost
Standard design	A	1.0	1.0	1.0	Standard
ST grid-tailored design (LV service)	B	0.8	0.8	0.8	Minimum
ST grid-tailored design (LV service + MV services)	C	0.8	0.8	2	Standard

Table 8. The grid and power converters specifications.

IGBT Losses

$$P = V_{CE} \cdot I_{ch(avg)} + r_{ch} \cdot I^2_{ch(rms)} + V_f \cdot I_{d(avg)} + r_d \cdot I^2_{d(rms)} \quad (1)$$

Channel losses *Body diode losses*

MV-Side Capacitor

$$C = \frac{S}{2 \cdot \pi \cdot f_{grid} \cdot \Delta V_{MVdC} \cdot V^2_{MVdC_{min}}} \quad (2)$$

Cooling System

$$CSPI\left[\frac{W}{K \cdot dm^3}\right] = \frac{1}{R_{th}[K/W] \cdot V[dm^3]} \quad (3)$$

$$V = \frac{P \cdot \left(\frac{1}{\eta} - 1\right)}{CSPI}(T_J - T_{amb}{}^{-1}) \quad (4)$$

LV-Side Capacitor

$$\Delta V_{pk-pk} = \frac{\Delta P_{pk-pk}}{2\pi f_H C^{dC}_{LV} V^{dC}_{LV}} \quad (5)$$

300 kW and the system is working at a nominal dc voltage of 700 V, a capacitance at least of 18 mF is suggested.

Additionally, for the dc/dc stage, the transformer design is considered. For the three different cases, the same transformer core with different litz wires is assumed. Thus, for the cost comparison of the transformer, only the iron amount is considered. The cost of the magnetics is evaluated by employing textbook formulas [23]: from the effective current, the wire area and the number of turns is evaluated. As design parameters, switching frequency, peak flux, and current density are considered constant, as is the core size. From the copper volume, it is possible to calculate the estimated costs [24]. From these assumptions, the volume of the copper is proportional to the processed power. Since the design is performed with the same dc voltage, the price of the copper is proportional to the effective current. For cases B and C, less iron is used on the transformer, leading to a cost reduction. The wires are selected according to the effective current, as shown in [15], which also provides more detail on the design of this stage.

Design Results Discussion

Because of the design, the normalized required semiconductor, cooling system volume, and capacitance for each design case are presented in Figure 5 for each stage of the ST. To compare the influence of the semiconductors selection on the ST design, two semiconductor modules from different manufactures were assumed for the MV side, due to their high performance: FF150R17KE4 (1.7 kV/150 A from Infineon Technology) and 2MBI75VA-170-50 (1.7 kV/75 A from Fuji Electric). The current rating of the Infineon Power Modules is twice that of the Fuji Electric, implying an underutilization of the former. Nevertheless, using the power module from Infineon, the current flowing through the channel is much smaller than the semiconductors' current rating, leading to an operation point with a small forward-drop voltage [$V_{CE(on)}$]. Consequently, the power dissipation is small, as well as the cooling system volume, as depicted in Figure 5(a). Note that the power semiconductor selection plays an important role in the ST design, affecting cost, efficiency, and volume (Figures 5 and 6). Apart from its own cost, the semiconductor selection influences the cooling system cost and volume. Hence, the tradeoff between these components must be considered. In this study, a heatsink building block with a cost of US$50 is assumed. These blocks are parallelized if more cooling

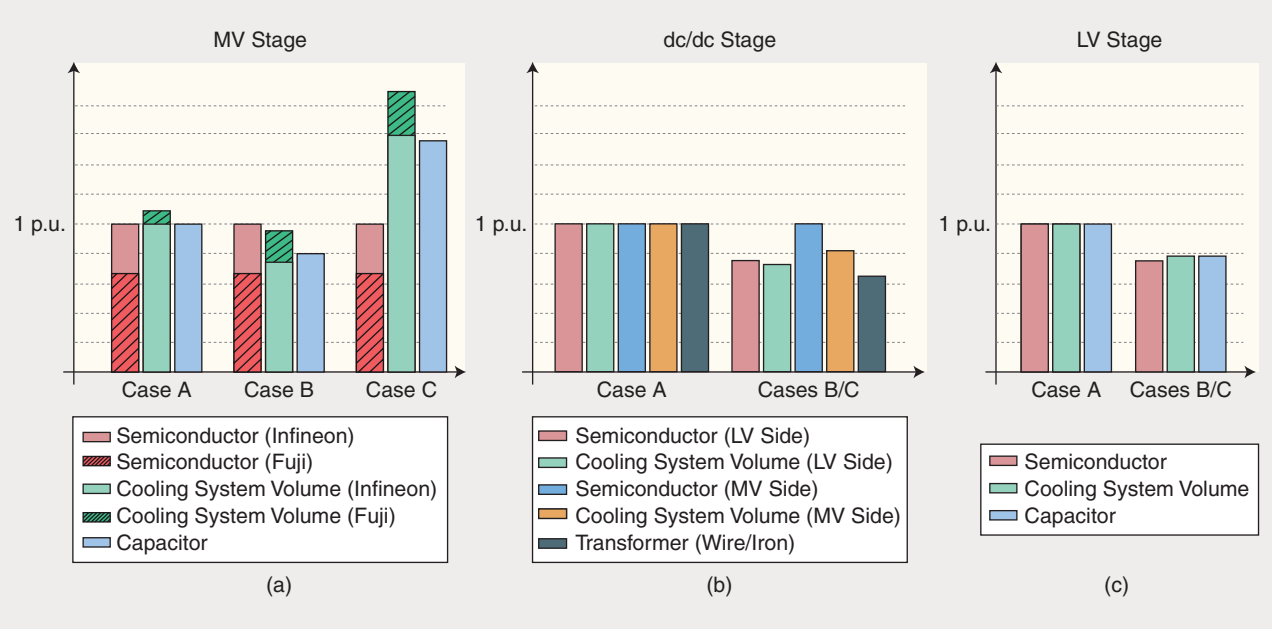

FIG 5 The ST design for three different cases: (a) the MV stage, (b) the dc/dc stage, and (c) the LV stage.

capability is required. For this case, an overall cost comparison of the MV stage considering those two different semiconductors is shown in Figure 6. Despite the high cooling system required by the Fuji Electric power modules [see Figure 5(a)], the semiconductors' price is considerably lower, compensating for the high investment in the cooling system. Therefore, the MV stage design using Fuji Electric is more economically viable.

Due to the higher power level in case C, the semiconductor is better used than in cases A and B. On the other hand, the amount of cooling is much higher, since the power dissipation is also higher. For the LV-side and dc/dc stages, the designs for cases B and C are the same, since the amount of processed power and voltage remains the same. As already mentioned, in case C, the saving cost from the LV side and dc/dc is invested on the MV stage. Considering the results obtained (illustrated in Figure 5), the cost savings are shared among the cooling system and capacitors, once the semiconductors of the MV remain the same. For this reason, a reduction of 20% of power in the LV and dc/dc stages allows an increase in MVA power of around 100% with respect to case A. Thus, for the assumed parameters, the MV stage can provide 2 MVA of apparent power, keeping the same overall system cost of case A; see Figure 7.

A Simulation Case Study of the Proposed GTDA

Depending on the grid needs, the ST can provide different services: local voltage support, voltage control in a specific bus, and power factor control at the HV/MV substation busbar. The simplest service it can provide is the operation under unity power factor. The LV-side converter produces the reactive power for the LV grid, and the MV converter can absorb only active power, reducing the reactive power burden of the MV grid. The ST injects reactive power to control the voltage at its busbar, or at a specific busbar in the grid. In a specific case, it can control the power factor at the HV/MV substation busbar, avoiding low power factor conditions (i.e., below 0.9 p.u.). However, the reactive power injection depends on the MV converter size and the active power request in the LV side (both ac and dc). The LV active power can be only partially regulated [6], but it affects the power quality in the grid. Instead, the size of the MV-side converter can be tailored to the MV grid to have better control margins.

Figure 8 depicts a practical example of an experiment described previously. A load flow simulation has been performed on a modified IEEE 34-bus test feeder. The grid voltage adopted is 10 kV, to match with the ST considered in this article. The ST absorbs 700 kW of active power, and the LV loads work with a power factor of 0.9 p.u. The ST injects reactive power to its maximum capability to support the voltage profile. If the ST is sized following the conventional transformer or SST design strategy (case A), the amount of reactive power injected is limited to 714 kVAR, which is not sufficient to keep the voltage at about 0.95 p.u. For case B, the power processed by the ST is lower than the case A applications. Thus, the amount of reactive power injected in the MV grid is lower, and no voltage support can be given (refer to the green line in Figure 8). With the proposed design approach in case C, the ST can be undersized in the LV and dc/dc stages, and the MV converter can be increased up to 2 MVA, without increasing the transformer costs. However, the benefits for the MV grid are clear. With higher reactive power capability, the ST can sustain the voltage profile

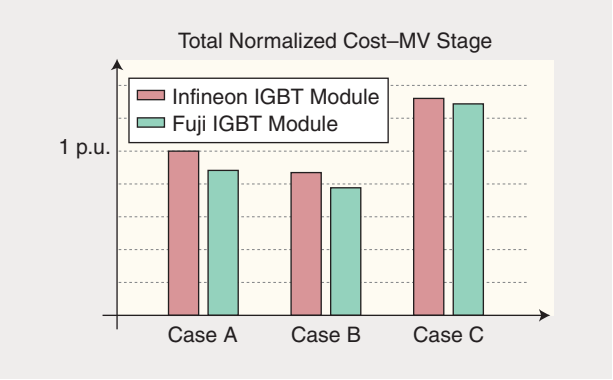

FIG 6 A cost comparison of the MV stage for different semiconductors' power modules.

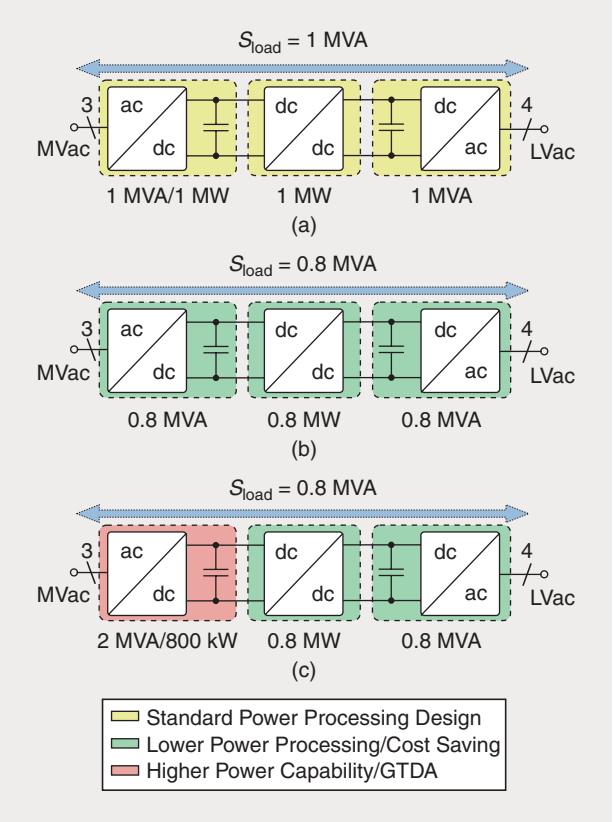

FIG 7 A block diagram of the ST considering the three different design approaches, highlighting the power processed by each stage: (a) case A, the standard design approach; (b) case B, the standard design plus the LV services to reduce the load consumption; and (c) case C, the proposed GTDA.

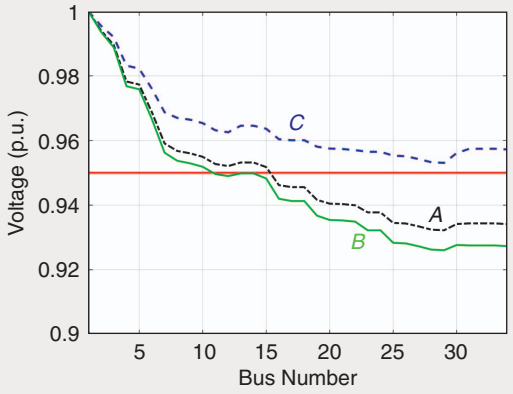

FIG 8 The voltage profile in the modified IEEE-34 bus feeder in the design case A (point-dot black line), case B (continuous green line), and case C (dotted blue line). The minimum voltage limits are marked (continuous red line, 0.95 p.u.).

Table 9. The specifications for the implemented prototype of the ST unit.

Parameters	Value
Maximum power	20 kW
Max ac voltage	1.4 kV RMS/50 Hz
Individual MVdc link	700 V
LVdc link	700 V
Isolation frequency	20 kHz

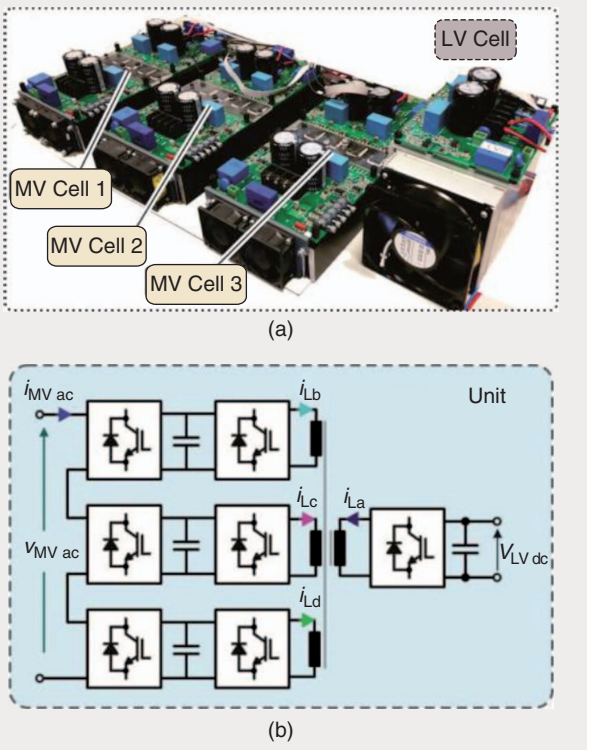

FIG 9 The implemented ST unit prototype based on the CHB and QAB converter and the experimental results obtained from it: (a) a photo of the prototype; (b) the topology of the implemented power stage.

above 0.95 p.u. in the whole grid, guaranteeing a good quality of the service.

Experimental Results of the ST

To evaluate experimentally the operation of the ST, a downscaled prototype has been developed and tested. Table 9 presents the specifications of the prototype, and Figure 9 shows the prototype and the topology. On the MV side, the cells of the CHB and QAB are assembled together and share the cooling system. A peak efficiency of 94.5% was obtained with IGBT IHW40N120. To reduce the switching and conduction losses, silicon carbide metal–oxide–semiconductor field-effect transistors could be used, allowing for an increase in efficiency up to 97.5% (with C2M0025120D devices).

Conclusions and Future Research Topics

In this article, the design of a three-stage ST is analyzed. The standard design flow for this system implies sizing each stage for the peak load request from the LV side. By exploiting the control functionality of the ST, however, a controllability margin exists to reshape the load profile, effectively decreasing the power-handling requirements from the LV and dc/dc stages. This feature is exploited by a GTDA, where the cost saved in the LV and dc/dc stage is reinvested in the MV stage, allowing it to process a greater amount of reactive power to guarantee MV voltage support. The GTDA allows an ST design that can supply the same grid as an SST but provides grid voltage support on the MV side at the same cost.

Acknowledgments

The research leading to these results received funding from the European Research Council (ERC) under the European Union's Seventh Framework Program (FP/2007-2013)/ERC Grant Agreement 616344—HEART.

About the Authors

Levy Ferreira Costa (lfc@tf.uni-kiel.de) received his B.S. degree in electrical engineering from the Federal University of Ceara, Fortaleza, Brazil, in 2010 and his M.S. degree in power electronics from the Federal University of Santa Catarina, Florianópolis, Brazil, in 2013. He is currently working toward his Ph.D. degree in power electronics at the Chair of Power Electronics at the Christian-Albrechts Universität zu Kiel University, Germany. From 2013 to 2014, he was an electrical design engineer at Schneider Electric, Brazil. His research interests include dc–dc converters, uninterruptible power system systems, and high-power converter systems.

Giovanni De Carne (gdc@tf.uni-kiel.de) received his bachelor's and master's degrees in electrical engineering

from "Politecnico di Bari" in Italy in 2011 and 2013, respectively. In 2013, he started working toward his Ph.D. degree at the Chair of Power Electronics at the Christian-Albrechts Universität zu Kiel, Germany. His Ph.D. work includes analysis of smart transformer features for electric distribution grid under the European Research Council grant project "Highly Reliable and Efficient Smart Transformer (HEART)." Currently, he is working on the Kopernikus project "New Energy Grid Structures for the German Energiewende–ENSURE."

Giampaolo Buticchi (gibu@tf.uni-kiel.de) received his master's degree in electronic engineering in 2009 and his Ph.D. degree in information technologies in 2013 from the University of Parma, Italy. He is now working as a postdoctoral research associate at the Christian-Albrechts Universität zu Kiel, Germany. His research area focuses on power electronics for renewable energy systems, smart transformer-fed microgrids, and reliability in power.

Marco Liserre (ml@tf.uni-kiel.de) received his M.S. and Ph.D. degrees in electrical engineering from the Polytechnic University of Bari, Italy, in 1998 and 2002, respectively. He is a full professor and head of the Chair of Power Electronics at the Christian-Albrechts Universität zu Kiel, Germany. He has published more than 300 technical papers (one-third in international peer-reviewed journals) and a book with second reprints that has also been translated into Chinese. He has been awarded a European Research Council Consolidator Grant, one of the most prestigious grants in Europe. He is member of the IEEE Industry Applications Society, Power Electronics Society, Power & Energy Society, and Industrial Electronics Society (IES) and has served all of these Societies in various capacities. He was founding editor-in-chief of *IEEE Industrial Electronics Magazine*, founding chair of the Technical Committee on Renewable Energy Systems, and IES vice-president for publications. He has received several IEEE awards.

References

[1] A. Ipakchi and F. Albuyeh, "Grid of the future," *IEEE Power Energy Mag.*, vol. 7, no. 2, pp. 52–62, Mar.–Apr. 2009.

[2] E. J. Coster, J. M. A. Myrzik, B. Kruimer, and W. L. Kling, "Integration issues of distributed generation in distribution grids," *Proc. IEEE*, vol. 99, no. 1, pp. 28–39, Jan. 2011.

[3] P. P. Barker and R. W. D Mello, "Determining the impact of distributed generation on power systems. Part I: Radial Distribution Systems," in *Proc. 2000 Power Engineering Society Summer Meeting*, Seattle, WA, 2000, pp. 1645–1656.

[4] M. Liserre, G. Buticchi, M. Andresen, G. De Carne, L. F. Costa, and Z. X. Zou, "The smart transformer: impact on the electric grid and technology challenges," *IEEE Ind. Electron. Mag.*, vol. 10, no. 2, pp. 46–58, June 2016.

[5] X. She, A. Q. Huang, and R. Burgos, "Review of solid-state transformer technologies and their application in power distribution systems," *IEEE J. Emerg. Sel. Topics Power Electron.*, vol. 1, no. 3, pp. 186–198, Sept. 2013.

[6] J. Wang, A. Q. Huang, W. Sung, Y. Liu, and B. J. Baliga, "Smart grid technologies," *IEEE Ind. Electron. Mag.*, vol. 3, no. 2, pp. 16–23, June 2009.

[7] J. W. Kolar, J. Huber, T. Guillod, D. Rothmund, F. Krismer, "Research Challenges and Future Perspectives of Solid-State Transformer Technology," presented at the 5th Int. Conf. Power Engineering Energy Electrical Drives, Riga, Latvia, 2015.

[8] G. De Carne, M. Liserre, and C. Vournas, "On-line load sensitivity identification in LV distribution grids," *IEEE Trans. Power Syst.*, vol. 32, no. 2, pp. 1570–1571, Mar. 2017.

[9] G. De Carne, G. Buticchi, M. Liserre, and C. Vournas, "Load control using sensitivity identification by means of smart transformer," *IEEE Trans. Smart Grid.*, Oct. 2016.

[10] G. De Carne, G. Buticchi, Z. X. Zou, and M. Liserre, "Reverse power flow control in a ST-fed distribution grid," *IEEE Trans. Smart Grid.*, Jan. 2017.

[11] G. Buticchi, G. De Carne, D. Barater, Z. Zou, and M. Liserre, "Analysis of the frequency-based control of a master/slave micro-grid," *IET Renew. Power Gener.*, vol. 10, no. 10, pp. 1570–1576, Nov. 2016.

[12] G. De Carne, G. Buticchi, M. Liserre, and C. Vournas, "Frequency-based overload control of smart transformers," in *Proc. IEEE Eindhoven PowerTech*, Eindhoven, The Netherlands, 2015, pp. 1–5.

[13] X. She, X. Yu, F. Wang, and A. Q. Huang, "Design and demonstration of a 3.6-kv 120-v/10-kva solid-state transformer for smart grid application," *IEEE Trans. Power Electron.*, vol. 29, no. 8, pp. 3982–3996, Aug 2014.

[14] C. Zhao, D. Dujic, A. Mester, J. Steinke, M. Weiss, S. Lewdeni-Schmid, T. Chaudhuri, and P. Stefanutti, "Power electronic traction transformer—medium voltage prototype," *IEEE Trans. Ind. Electron.*, vol. 61, no. 7, pp. 3257–3268, July 2014.

[15] L. Costa, G. Buticchi, and M. Liserre, "Quad-active-bridge dc-dc converter as cross-link for medium voltage modular inverters," *IEEE Trans. Ind. Appl.*, vol. 53, no. 2, pp. 1243–1253, Mar.–Apr. 2017.

[16] J. D. Luze, "Distribution transformer size optimization by forecasting customer electricity load," in *Proc. 2009 IEEE Rural Electric Power Conf.*, Fort Collins, CO, 2009, pp. C2–C2-6.

[17] Z. Wang and J. Wang, "Review on implementation and assessment of conservation voltage reduction," *IEEE Trans. Power Syst.*, vol. 29, no. 3, pp. 1306–1315, May 2014.

[18] K. P. Schneider, J. Fuller, F. Tuffner, and R. Singh. (2010, July). Evaluation of conservation voltage reduction (CVR) on a national level. U.S. Department of Energy. Oak Ridge, TN. Tech. Rep. PNNL-19596. [Online]. Available: http://www.pnl.gov/main/publications/external/technical_reports/PNNL-19596.pdf

[19] J. V. Milanovic, K. Yamashita, S. Martínez Villanueva, S. Djokic, and L. M. Korunović, "International industry practice on power system load modeling," *IEEE Trans. Power Syst.*, vol. 28, no. 3, pp. 3038–3046, Aug. 2013.

[20] H. Farhangi, "The path of the smart grid," *IEEE Power Energy Mag.*, vol. 8, no. 1, pp. 18–28, Jan.–Feb. 2010.

[21] U. Drofenik, G. Laimer, and J. W. Kolar, "Theoretical converter power density limits for forced convection cooling," in *Proc. Int. Power Conversion Intelligent Motion Europe Conf.*, Nuremberg, Germany, June 7–9, 2005, pp. 608–619.

[22] R. Teodorescu, M. Liserre, and P. Rodriguez, *Grid Converters for Photovoltaic and Wind Power Systems*. Hoboken, NJ: Wiley, 2011.

[23] M. K. Kazimierczuk, *High-Frequency Magnetic Components*. Hoboken, NJ: Wiley, 2009.

[24] Nasdaq. Copper: latest price and chart for high grade copper. [Online]. Available: http://www.nasdaq.com/markets/copper.aspx

PEM